Marine Genomics 27 (2016) 75–83

Contents lists available at ScienceDirect

Marine Genomics

Cells to Shells: The genomics of mollusc exoskeletons

Calcium mobilisation following shell damage in the Pacific oyster, *Crassostrea gigas*

J.K. Sillanpää [a,*], K. Ramesh [b], F. Melzner [b], H. Sundh [a], K. Sundell [a]

[a] Fish Endocrinology Laboratory, Department of Biology and Environmental Sciences, University of Gothenburg, Gothenburg, Sweden
[b] Helmholtz Centre for Ocean Research GEOMAR, Kiel, Germany

ARTICLE INFO

Article history:
Received 30 November 2015
Received in revised form 18 February 2016
Accepted 2 March 2016
Available online 16 March 2016

Keywords:
Biomineralisation
Calcium
Hemocytes
Hemolymph
Molluscs
Crassostrea

ABSTRACT

Shell growth of oysters requires calcium uptake from the environment and transport to the area of shell formation. A shell regeneration assay in combination with radiolabelled calcium was used to investigate uptake and distribution of calcium to different tissues and hemolymph fractions in Pacific oysters, *Crassostrea gigas* (Bivalvia, Ostreoida). Oysters were notched at the shell margin and subsequently sampled for hemolymph and grading of shell regeneration during a two week experimental period. Half of the oysters were additionally exposed to ^{45}Ca and sampled for hemolymph and tissues. Total plasma calcium concentrations increased in notched oysters compared to controls on 1, 2 and 7 days after notching. A decrease in plasma calcium levels was apparent on day 4, for both total and ionic calcium. The shell regeneration assay in the notched oysters resulted in a visible deposition of $CaCO_3$ onto the regenerate from day 7 onwards. This was coinciding with an increased uptake of total calcium on days 11 and 14 as well as free, i.e. ionic and ligand-bound calcium, on day 14. At day 1, notching also increased calcium uptake into the mantle tissues, in areas above the notch and near the hinge. During the experiment, both the total hemocyte count and the number of granulocytes increased in notched compared to control oysters. The present study suggests that induced shell damage results in a dynamic regulation of the calcium uptake from the environment and the distribution of calcium within the body, starting directly after notching. Increases in both total calcium concentrations and uptake rates coincided with the visible depositions of $CaCO_3$ on the regenerate shell. *C. gigas* was found to transport calcium mainly in the ionic form in the hemolymph, with only minor parts being bound to proteins or smaller ligands. Hemolymph measurement also revealed that *C. gigas* is able to regulate the extracellular concentrations of calcium and potassium. The changes in plasma calcium concentrations and speciation, concomitant with increases in granulocytes indicate that multiple calcium transport processes are activated after induced shell damage.

1. Introduction

Molluscs have a long evolutionary history and are one of the most successful animal phyla. Their evolutionary efficacy can partly be credited to the existence of their calcified shell, a structure that provides protection and support to the soft bodied organisms (Marin and Luquet, 2004). In addition to offering protection, valve closure plays a role in maintaining homeostasis by temporarily preventing ion exchange between the hemolymph and external media (Burton, 1983). The shell may further act as reservoir of ions, such as calcium and carbonate, during periods of excess demand e.g. acidosis, food deprivation and vitellogenesis (Jokumsen and Fyhn, 1982; Matozzo and Marin, 2007).

The main epithelia responsible for maintaining homeostasis and regulating the uptake of ions are the mantle, gills, gut and kidneys (Jodrey, 1953; Horiguchi, 1958; Potts, 1967; Rousseau et al., 2003; Fan et al., 2007). The mantle separates the body from the shell and is responsible for shell formation. It secretes the periostracum, as well as proteins, glycoproteins and polysaccharides which function as the organic matrix for biomineralisation (Joubert et al., 2010; Xiang et al., 2014). The matrix is suggested to initiate, regulate and inhibit growth and orientation of the calcium carbonate ($CaCO_3$) crystals and thereby control shell structure (Zhang and Zhang, 2006; Suzuki et al., 2009; Miyazaki et al., 2010).

Transport of ions by the gills and the mantle is an essential function for shell formation. Although the process of shell development is a well-studied subject in molluscs (Kniprath, 1980; Eyster, 1983; Medaković, 2000; Hohagen and Jackson, 2013), understanding of the calcium transport mechanisms is not comprehensive. The general view of bivalve shell formation suggests that biomineralisation occurs via precipitation of $CaCO_3$ crystals in the organic matrix from a supersaturated solution of $CaCO_3$ in the extrapallial space i.e. the compartment between the outer mantle epithelium (OME) and the shell (Wheeler and Sikes, 1984;

* Corresponding author at: Fish Endocrinology Laboratory, Department of Biology and Environmental Sciences, University of Gothenburg, PO Box 463, S-405 30 Gothenburg, Sweden.
E-mail address: kirsikka.sillanpaa@bioenv.gu.se (J.K. Sillanpää).

http://dx.doi.org/10.1016/j.margen.2016.03.001
1874-7787/

Levi-Kalisman et al., 2001; Joubert et al., 2010; Marie et al., 2011; Marin et al., 2012). This hypothesis has been questioned by models suggesting that too large volumes of such solutions would be required for this to be feasible (Addadi et al., 2006) and that the extrapallial fluid is undersaturated with regard to $CaCO_3$ (Misogianes and Chasteen, 1979; Heinemann et al., 2012). Alternative models suggest that the formation of $CaCO_3$ crystals occurs outside of the extrapallial space and that the calcium carbonate particles are then transported to and/or released at the site of shell formation. In the Eastern oyster, *Crassostrea virginica*, granulocytes containing $CaCO_3$ crystals have been reported in the hemolymph (Mount et al., 2004). The granulocytes were observed at the site of calcification and increased in abundance in relation to other hemocytes during induced shell regeneration. Recent studies suggest that precipitation of amorphous $CaCO_3$ also occurs inside mantle epithelial cells (Xiang et al., 2014) and that vesicles containing $CaCO_3$ crystals are deposited onto the newly formed organic matrix secreted by the OME cells (Johnstone et al., 2015).

Thus, the current view of shell formation in marine oysters suggests that both the mantle and the hemocytes play important and specific roles during the shell forming process. The required calcium is suggested to be absorbed by the gills and the mantle tissue and transported in the hemolymph and/or across the mantle epithelium to the site of biomineralisation (Marin and Luquet, 2004; Fan et al., 2007; Marin et al., 2012). Calcium can be transported in several ways; in its ionic form, bound to ionic complexes, bound to peptides or proteins or in the form of amorphous particles or crystals intra- or extracellularly (Coimbra et al., 1993; Nair and Robinson, 1998; Mount et al., 2004; Marin et al., 2012; Xiang et al., 2014). However, there is still lacking information regarding the roles of the different compartments that are important in calcium uptake and transport during shell formation. Therefore the aims of the present study are to (i) assess the distribution of different calcium species in the hemolymph of *Crassostrea gigas* during shell repair (ii) investigate the pathways for calcium uptake following shell damage and (iii) investigate the role of hemocytes in the transport of calcium to the area of shell repair.

2. Materials & methods

2.1. Oyster collection and experimental design

Wild adult *C. gigas* were randomly collected from the intertidal zone at Sylt (Königshafen near List, pH 7.9–8.1), Germany (55°1′52.4172″N, 8°25′37.005″E) on 26 November 2014. The oysters (mean shell length: 11.47 ± 0.19 cm) were transferred on ice to GEOMAR, Kiel, Germany and held in a 100 L tank with artificial seawater (Instant Ocean, 28.3‰) at 12 °C, for 2 days prior to transport to the aquaria facilities at the Department of Biology and Environmental Sciences, University of Gothenburg, Sweden. The oysters were randomly divided into twelve identical 22 L plastic aquaria, 12 oysters/aquaria, filled with 16 L of artificial seawater at 10 °C. The aquaria were oxygenated using compressed air which also maintained a pH of 7.85 ± 0.01 (Table 1) for the duration (14 days) of the experiment. The oysters were not fed during the experiment, and the water was changed every other day to avoid accumulation of metabolic wastes and faecal excretion (see Section 2.2 and Table 1). Half of the animals (72) were used in ^{45}Ca labelling experiment while the other half was used for hemocytes characterisation and hemolymph calcium speciation studies. V-shaped notches were drilled in close proximity to the adductor muscle using a multifunctional Dremel drill with a circular burr of 2.5 cm diameter as previously described in Mount et al. (2004) in 36 oysters to be ^{45}Ca exposed and to 36 "cold" oysters. At the time points: 1, 2, 4, 7, 11 and 14 days after notching, 2 animals from each aquarium of the non-radiolabelled groups were sampled for hemolymph (6 cold-notched, 6 cold-control) and 2 animals from each aquarium of the ^{45}Ca-labelled groups for hemolymph and tissues (6 ^{45}Ca-notched and 6 ^{45}Ca-control).

Table 1
Water parameters during the duration of the cold experiment.

Day	NH_4 (mg/L)	pH	T (°C)	Salinity(psu)	Osm
0	0.2 ± 0.00	7.85 ± 0.00	10	28.3	864
1	0.3 ± 0.03	7.83 ± 0.01	10	28.3	
2	0.6 ± 0.00	7.82 ± 0.00	10	29.1	
3	0.1 ± 0.00	7.85 ± 0.00	10	29.1	
4	<0.05	7.82 ± 0.00	10	29.1	882
5	0.1 ± 0.00	7.80 ± 0.01	10	29.1	
6	<0.05	na	10	29.1	
7	0.4 ± 0.00	7.85 ± 0.00	10	28.6	
8	<0.05	7.88 ± 0.00	10	28.6	
9	0.1 ± 0.00	7.85 ± 0.00	10	29.3	
10	<0.05	7.91 ± 0.00	10	29.3	895
11	0.1 ± 0.00	7.82 ± 0.00	10	29.3	
12	<0.05	7.90 ± 0.01	10	29.8	
13	na	na	10	29.8	921
14	0.1 ± 0.00	7.86 ± 0.00	10	29.8	

2.2. Water chemistry measurements

The artificial seawater, Instant Ocean (28.3‰, $[Ca^{2+}]$ 7.7 mM, $[Na^+]$ 456 mM, $[K^+]$ 5.8 mM, analysed by flame emission photometry, with LiCl as internal standard (Eppendorf AG, Hamburg, Germany; model ELEX 6361)) was prepared in two 1 m^3 closed, header tanks, in order to last for water changes every other day throughout the experiment. Water temperature and salinity (Testo 240 Conductivity meter, Germany) were measured from the header tank supplying the exposure aquaria. pH (Metronohm 744 pH meter, Switzerland) and ammonia concentrations (JBL NH_4 test kit, Germany) were measured daily in the 6 aquaria containing non-radiolabelled Instant Ocean and osmolality was assessed with Micro Osmometer 3300 (Advanced Instruments Inc., Massachusetts, USA) at 4 time points (Table 1). An additional mixing of header tank water at day 11 (cold) was necessary due to a leakage. Thus, water change at days 11 and 13 of the cold experiment and at day 11 of the ^{45}Ca labelling experiment was made from freshly prepared artificial seawater.

2.3. Shell repair analyses

Shell repair was assessed by classifying the degree of regeneration at the site of notching by ocular examination, without magnification, according to a shell repair classification using 4 stages (Cho and Jeong, 2011; Hüning, 2013; Table 2). Briefly, in the first stage (stage I) no signs of shell repair were visible. The next stage (stage II) was defined as the initial deposition of an organic layer. Stage III was characterised by increased organic sheet deposition and tanning of the organic sheet to form the periostracum. The final stage (stage IV) was identified by deposition of $CaCO_3$ onto the organic layer as observed by an overall change in colour, scattering of white deposits and increased sheet rigidity.

2.4. Hemocyte characterisation

From each oyster, 300 μL of hemolymph was drawn from the adductor muscle using a 60 mm 23 gauge needle affixed to a sterile 1 mL plastic syringe coated with a calcium-free artificial seawater

Table 2
Classification of repair stages according to the observed changes.

Stage	Description
I	No visible components of shell-repair process
II	Organic matter formation
III	Tanning of organic layer and increase in surface area of organic layer
IV	$CaCO_3$ deposition visible

(918 ± 5 mOsm; Cavanaugh, 1975). An additional 1 mL was drawn from the muscle for assessing calcium speciation in hemolymph (see 2.5). For cell population characterisation, the hemolymph was fixed in 300 μL 6% formalin in filtered (0.2 μm) Instant Ocean (28.3 ‰). Samples were analysed using a BD Accuri C6 flow cytometer, and BD Accuri C6 software (Version 1.0.264.21) was used to analyse samples. A bead set standard provided by BD Biosciences was used and found to be within limits set by the manufacturer of the flow cytometry. A total volume of 15 μL of the fixed hemolymph sample was used to analyse changes in the hemocyte populations. A core size of 11 μm and flow rate of 48 μL/min was applied for measurements. Analyses were performed by gating cell populations in the log forward scatter (FSC) vs log side scatter (SSC) plots according to results from previous studies on oysters, including *C. gigas* (Hégaret et al., 2003a, 2003b; Lambert et al., 2007).

2.5. Hemolymph ion concentrations and calcium species

Hemolymph (1 mL) was centrifuged for 10 min at 2000*g* (4 °C) to separate the cells from the plasma and stored at −80 °C until analysis. Total plasma calcium (Ca_T), sodium and potassium were measured from whole plasma using a flame emission photometer, with LiCl as internal standard (Eppendorf AG, Hamburg, Germany; model ELEX 6361).

Size dependent fractionation using ultrafiltration and ion selective electrodes was used to separate the chemically different calcium species (ionised Ca, complex bound Ca and protein bound Ca; Fig. 1). In order to separate the calcium bound to proteins >30 kDa (Ca_P) from the ionic calcium and calcium bound in complexes and to ligands ≤30 kDa, together making up the filterable or free calcium fraction (Ca_F), 400 μL of hemolymph plasma was filtrated using an Amicon MPS-1 ultrafiltration device (MA, USA) with 14 mm YMT-filtrate membranes (cut-off size 30 kDa) through centrifugation at 2000*g* (Beckman Coulter Allegro X-15R, CA, USA) for 1 h at room temperature (Renwrantz et al., 1998). The ability of these membranes to retain hemolymph proteins from *C. gigas* was tested using Pierce™ BCA Protein Assay Kit (Thermo Scientific) prior to the experiment and resulted in a 93.6 ± 0.64% retention of the peptides/proteins. Ionised calcium (Ca_I) in whole plasma was analysed using a Convergy ISE Comfort M05 electrolyte analyser (Convergent Technologies, Germany).

Both Ca_T and filtrates, i.e. the Ca_F, were analysed for total calcium concentrations using the flame emission photometer. The fraction of calcium bound to proteins >30 kDa, i.e. the Ca_P, was calculated as:

$$Ca_P = Ca_T - Ca_F$$

Calcium concentration of hemocytes contained in 1 mL of hemolymph (Ca_H) was assessed using the cells initially separated from the hemolymph samples. The cells were re-dissolved in 100 μL distilled water, vortexed and measured for total calcium using the flame emission photometer as described for the plasma samples.

2.6. Calcium mobilisation from the environment

To investigate the route of calcium uptake from the environment during shell regeneration, 72 oysters, of which half were notched (36 ^{45}Ca-notched and 36 ^{45}Ca-control) were exposed to radiolabelled ^{45}Ca. 1.6 MBq ^{45}Ca (specific activity 409.71 MBq/mg PerkinElmer, MA, USA) was added to each tank at day 0 and subsequently after each water change every other day throughout the experiment. Water samples were collected concurrent with each water change. At each sampling day, 2 oysters from each aquarium (6 ^{45}Ca-notched and 6 ^{45}Ca-control) were sampled for mantle tissue as outlined in Fig. 1. Additionally, tissue samples from adductor muscle and gills were collected, as well as 1 mL hemolymph, from each oyster. All tissue samples were weighed with the precision of 0.01 g.

Tissues were solubilized in 1 mL of Soluene-350 (PerkinElmer) for 3 h at 60 °C. 200 μL of 30% (*w*/*v*) hydrogen peroxide was added to the solubilized samples in two 100 μL additions during shaking, following which the samples were incubated at 60 °C for an additional 30 min. 10 mL of scintillation fluid (Hionic-Fluor, Perkin Elmer) was added to each sample. The samples were incubated in darkness at room temperature for 1 h and radioactivity was measured in a liquid scintillation counter (Wallac 1409 Liquid Scintillation β-Counter, Turku, Finland).

Hemolymph samples from the ^{45}Ca labelling experiment were collected and stored at −80 °C as previously described for non-labelled samples. 300 μL of plasma was filtered using the Amicon MPS-1 ultrafiltration device with YMT-membranes, and the resulting filtrate was collected as described above. 100 μL of the whole plasma sample ($^{45}Ca_T$) as well as the filtrate (≤ 30 kDa; $^{45}Ca_F$) was analysed for ^{45}Ca activity using the same scintillation fluid and β-counter as for

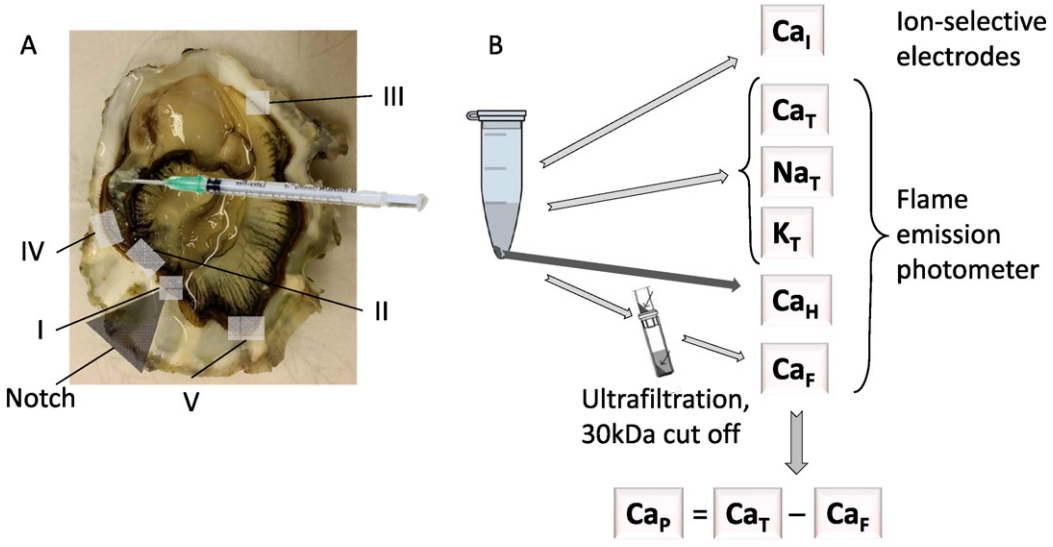

Fig. 1. A. Locations of mantle tissue samples, area of notching and hemolymph sampling from the adductor muscle. B. Flow diagram of separation and methods to analyse the different calcium species in the hemolymph.

tissue samples. In this experiment, the filter papers were collected to measure the amount of ^{45}Ca bound to proteins >30 kDa ($^{45}Ca_P$). The YMT-filters were solubilized in 10 mL of a specific solubilizing scintillation fluid, Filter count (Perkin Elmer, MA, USA). To measure the amount of ^{45}Ca transported inside the hemocytes ($^{45}Ca_H$), previously separated cells (from 1 mL of hemolymph) were solubilized in 1 mL of a 4:1 mixture of Soluene-350:MQ water for two hours at 60 °C. Thereafter, 10 mL of HionicFluor was added and samples were analysed using the β-counter. Water samples were analysed for ^{45}Ca activity by adding 10 mL Hionic-Fluor to 1 mL of sample and activity assessed in the β-counter.

2.7. Data analysis and statistics

Results from ^{45}Ca liquid scintillation counting, disintegrations per minute (DPM), were corrected for the radioactive decay by calculating the fraction of remaining activity using Eq. (1) (Kahl et al., 2012)

$$\text{Fraction Remaining} = e^{\left(-0.693/t_{1/2}\right)*\text{time}} \quad (1)$$

where $t_{1/2}$ is the half-life of the isotope (162.7 days for ^{45}Ca), and time refers to the number of days after the manufacturer reference date.

The specific activity of ^{45}Ca ($MBq*mol^{-1}$) in the water was calculated for each aquarium and time point as:

$$\frac{^{45}\text{Ca activity measured in each water sample } \left(MBq*l^{-1}\right)}{\text{total calcium concentration in the water } \left(mol*l^{-1}\right)}.$$

Calcium uptake ($mol*l^{-1}$) to the different calcium hemolymph speciations: $^{45}Ca_T$, $^{45}Ca_P$, $^{45}Ca_F$ and $^{45}Ca_H$, was calculated as:

$$\frac{^{45}\text{Ca activity measured } \left(MBq*l^{-1}\right)}{\text{specific activity of the water } \left(MBq*mol^{-1}\right)}$$

and calcium uptake from the environment to the different tissues ($mol*g^{-1}$) was calculated as:

$$\frac{^{45}\text{Ca activity measured } (MBq*g^{-1})}{\text{specific activity of the water } \left(MBq*mol^{-1}\right)}.$$

Normality and homogeneity of variances were tested for the residuals and predicted values in a general linear model (GLM). Data not passing the test were transformed and passed using log 10 transformation. A nested, mixed linear model, using treatment and time as fixed factors and tanks nested within treatment, was used to analyse differences in hemolymph calcium species and calcium mobilisation. In case of significant interactions between factors, further post hoc analysis was performed using Bonferroni corrected multiple pair-wise comparisons. The statistical analyses were performed using IBM SPSS 22 (SPSS Inc., Chicago, Illinois). All data are expressed as means ± SEM and $p < 0.05$ values were regarded as significant.

3. Results

3.1. Shell repair observations

On day 1, no organic deposits to seal the damaged shell area could be observed on any of the notched oysters. Stage II of shell recovery, denoting first organic deposits, was observed on day 2, with organic material covering 2–6% of the damaged area. Stage III, tanning of the organic layer, was first noted on day 4. Stage III was observed on 18–34% of the recently deposited organic sheets on the oysters on day 7, while half of the animals were already depositing $CaCO_3$ onto the organic sheets (Stage IV). By day 11 all the animals were in stage IV, i.e. depositing $CaCO_3$ on the organic layer (Fig. 2).

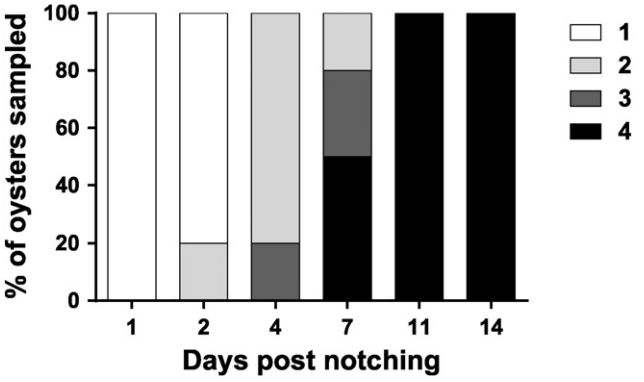

Fig. 2. Stages of shell repair observed using ocular examination and assessed according to degree of shell repair classified using a four grade scale: 1 = No visible components of shell-repair processes; 2 = Organic matter formation; 3 = Tanning of organic layer and increase of organic area surface; 4 = Visible $CaCO_3$ crystal deposition. N = 6.

3.2. Hemocyte characterisation

Flow cytometry of hemolymph cells revealed changes in both total hemocyte count and hemocyte type (Fig. 3). There was an overall time effect in the total hemocyte count, with a peak on day 7 and a second increase on day 14 (Fig. 3A). This pattern was reflected in the total number of granulocytes in the notched oysters, which significantly increased in abundance on day 7 when compared to the beginning of the experiment (day 1; Fig. 3B). This increase in the number of granulocytes was also apparent when comparing the number of granulocytes between control and notched oysters, where all time points except day 1 showed higher granulocyte counts in notched compared to control oysters (Fig. 3B). Thus, following shell damage, the percentage of granulocytes in the hemolymph of notched oysters increased from below 1% at day 1, to ca. 5% at day 14. The total hemocyte count was not statistically different between the two groups due to high variability, although there was a tendency ($p = 0.059$) towards higher cell numbers in notched oysters compared to control.

3.3. Hemolymph ion concentrations and calcium species

Plasma sodium levels, ranging between 385 mM and 431 mM (mean value per treatment and sampling time), were close to environmental concentrations (456 mM) throughout the experiment (Fig. 4D). A significantly higher Na level was observed in the notched compared to control oysters at day 2, and a slightly higher level of Na was seen in the control oysters at day 1 compared to day 14 (Fig. 4D). Plasma potassium levels, on the other hand, ranging from 10.4 to 13.3 mM in control oysters and 8.8–11.0 mM in the notched, were consistently above the environmental concentrations (5.8 mM). Potassium levels were also affected by the treatment, with lower levels in the notched oysters at days 4, 7 and 14 (Fig. 4E).

Concentrations of the chemically different forms of calcium (Ca species) present in the hemolymph were measured in the non-labelled hemolymph samples. The control oysters experienced a slight increase in Ca_T from 9.0 ± 0.23 mM to 9.3 ± 0.15 mM as well as in Ca_I from 7.4 ± 0.36 mM to 8.3 ± 0.14 mM, from day 1 to day 14 (Fig. 4A, B). Conversely, in the notched oysters there were no significant differences in Ca_T between the time points except for day 4, when there was a transient decrease of approximately 1.1 mM (Fig. 4A). The Ca_I concentrations in the notched oysters were higher at days 11 and 14 compared to days 1 and 2 and similar to the Ca_T, there was a transient decrease in Ca_I at day 4 (approximately 1.6 mM; Fig. 4B). Ca_T was further higher in the notched compared to control oysters on days 1, 2

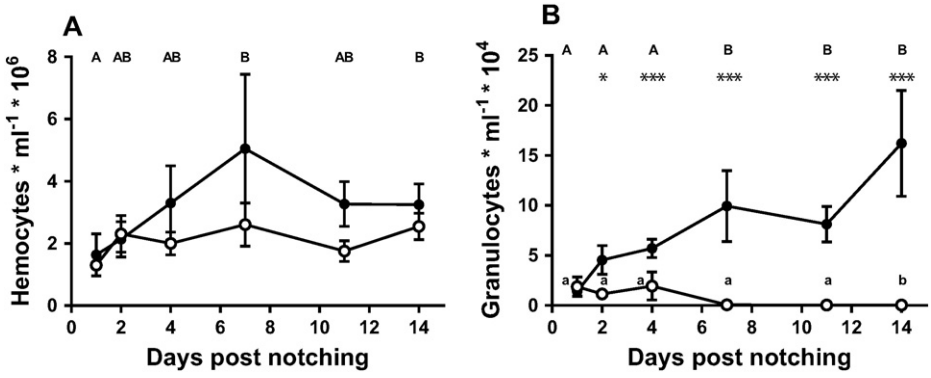

Fig. 3. The total number of hemocytes (A) and granulocytes (B) in the hemolymph of *Crassostrea gigas* for 14 days following shell injury. Error bars indicate ± standard error of mean (n = 6). Asterisks indicate treatments that are significantly different from controls ($p < 0.05$; Bonferroni multiple pairwise comparison). Values with dissimilar letter indicate significant difference between time points ($p < 0.05$; for A. Bonferroni multiple pairwise comparison, for B. GLM).

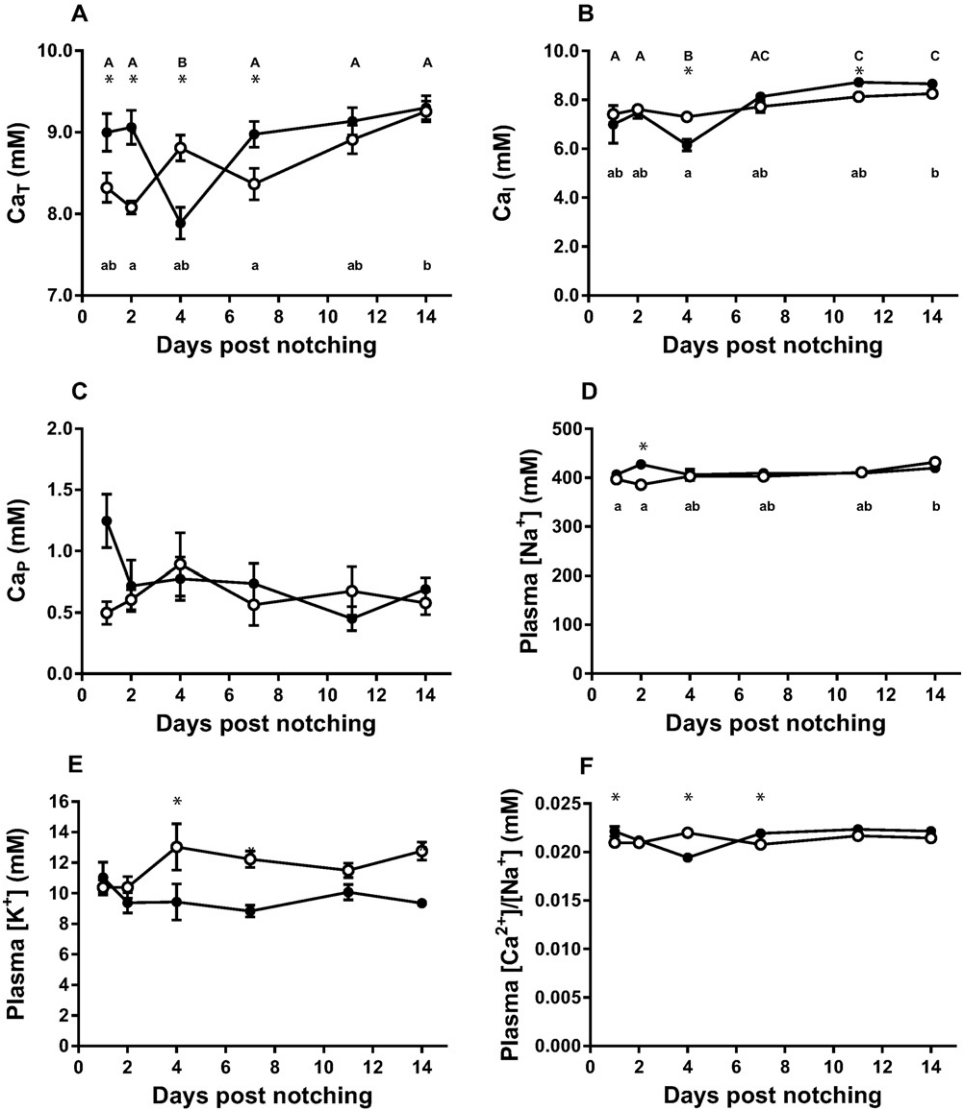

Fig. 4. Hemolymph ion concentrations (mM) of notched and control oysters with time. The different calcium species of the hemolymph (A–C) are assessed using ion selective electrodes for Ca_I and flame emission photometer for C_T. Total sodium and potassium concentrations (D, E) are measured using flame emission photometer. A) total plasma calcium, Ca_T; B) ionic plasma calcium, Ca_I; C) calcium bound to proteins >30 kDa, Ca_P; D) total sodium concentration; E) total plasma potassium concentration; F) ratio between total plasma calcium and total plasma sodium. Values are means ± standard error of the mean (n = 6) and asterisks denotes significant differences between treatment groups ($p < 0.05$; Bonferroni multiple pairwise comparison). Values with dissimilar letter indicate significant difference between time points, upper case indicates notched animals and lower case control (($p < 0.05$; Bonferroni multiple pairwise comparison).

and 7 and lower on day 4, whereas Ca_I was significantly lower in notched oysters compared to control on day 4 and higher on day 11. Ca_P, the fraction of calcium bound to proteins >30 kDa, was not affected by either treatment or time. Referring to the major cation of the plasma, sodium, the ratio of Ca_T to plasma sodium was higher at days 1 and 7 and lower at day 4, in notched compared to control oysters (Fig. 4F).

Ca_H, i.e. the calcium concentrations associated with the hemocytes, were highly variable with an overall effect of time and treatment, Ca_H concentrations were higher in control compared to notched oysters with an overall increase in Ca_H with time (Fig. 5).

3.4. Uptake and distribution of radiolabelled ^{45}Calcium

In order to study the uptake and distribution of calcium in the different tissues and the different hemolymph calcium species, notched and control oysters were exposed to artificial seawater containing ^{45}Ca. The average activity of ^{45}Ca was 0.121 ± 0.011 MBq∗L^{-1} in experimental aquaria containing notched oysters and 0.125 ± 0.014 MBq∗L^{-1} in control aquaria, rendering an average specific activity of 0.017 MBq/mmol Ca in control tanks (ranging from 0.006 to 0.03) and 0.016 MBq/mmol in the tanks containing the notched oysters (ranging from 0.007 to 0.03).

During the experimental exposure, ^{45}Ca uptake in the different mantle tissue sections, 1, 2, 3, 4 and 5 (see Fig. 1 for anatomical explanation) as well as in gills and muscle tissue increased in both notched and control oysters with time (Table 3). Significant differences were found between days 1 and 14 in Sections 2, 4 and 5, and between days 2 and 14 in tissue sections 1 and 3 (Table 3). For mantle tissue from sections 2 and 3, the overall treatment effect revealed a higher ^{45}Ca uptake in notched compared to control oysters. For the adductor muscle, ^{45}Ca uptake increased during the course of the experiment and was significantly higher in notched compared to control oysters (Table 3).

^{45}Ca uptake and accumulation into the different hemolymph species, $^{45}Ca_T$, $^{45}Ca_P$ and $^{45}Ca_F$, increased with time in both control and notched oysters (Fig. 6A–D). $^{45}Ca_T$ was elevated in the notched oysters compared to the controls at days 11 and 14, by 17% and 22%, respectively (Fig. 6A). This pattern was reflected in $^{45}Ca_F$ on day 14 (Fig. 6C). The uptake and accumulation of ^{45}Ca in the $^{45}Ca_H$ or $^{45}Ca_P$ did not differ between the treatments at any time points (Fig. 6B, D).

4. Discussion

In the present study, notching of the oyster shell was used as a shell regeneration assay to investigate the mobilisation of calcium during shell repair. The focus was placed on calcium uptake and transport in the hemolymph to the area of repair. Induced shell damage increased calcium levels in the plasma at day 1 following notching. This calcium was mainly in the form of ionic and ligand-bound calcium. The tracer experiments revealed increased accumulation of radiolabelled free calcium in the hemolymph also at later time points in the experiment. This occurred after $CaCO_3$ formation on the regenerate was observed, suggesting an increased turn-over rate of calcium after 11–14 days from notching. The different sections of mantle tissue varied in their response to induced shell damage. There was an increased calcium uptake in the upper mantle close to the notch and in the lower mantle on the dorsal side close to the shell hinge, directly after notching. The number of circulating hemocytes, as well as the number of granulocytes, increased during the experiment, suggesting that these cells proliferate in response to shell damage.

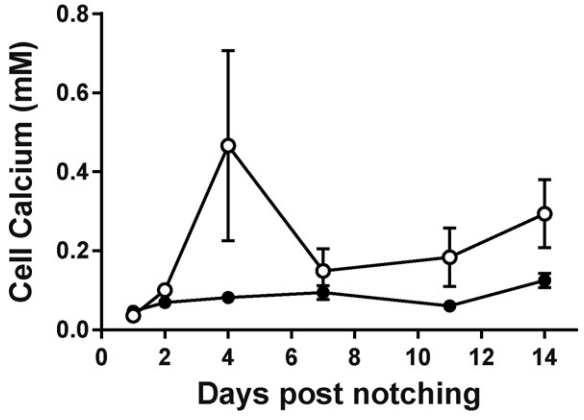

Fig. 5. Calcium concentrations inside hemocytes (mM) of notched and control oysters with time. The calcium concentrations are assessed using flame emission photometer. Values are means ± standard error of the mean (n = 6).

Non-radioactively labelled notched oysters were observed to have higher total and ionic plasma calcium immediately after notching on days 1 and 2, followed by a drop on day 4, compared to control oysters. As calcium is proposed to be taken up as ionic calcium (Fan et al., 2007), this indicates that the initial elevated plasma levels are due to increased calcium uptake following shell damage. This is supported by the increased uptake of calcium, traced as radiolabelled calcium, in the ^{45}Ca-notched animals on day 2. However, there was no change in calcium uptake at day 4, despite a clear drop in the plasma total and ionic calcium levels on the same day. It is therefore hypothesised that an increased rate of incorporation of calcium into the regenerating shell, without a corresponding increase in calcium uptake rate, may be the reason for this transient decrease in plasma total and ionic calcium levels. At day 4, organic deposits were observed in all the animals except one and at day 7, $CaCO_3$ deposits were observed (without magnification) in half of the oysters. During regeneration of oyster shells under warmer conditions (14–18 °C) the first $CaCO_3$ deposits have been noted to occur 48 h after the induced shell damage (SEM; Mount et al., 2004; Tejaswi Yarra personal communication). The first deposits are likely to occur more rapidly at higher temperatures and the exposure temperature is thus one factor that can explain the discrepancies in time of first shell deposit between the present and previous studies. In addition, the use of SEM for crystal detection is a more sensitive method than ocular examination, and small deposits of $CaCO_3$ crystals are likely to be present, but undetected, also prior to day 7 in the present study. After the transient decrease at day 4, the ionic calcium concentrations increased steadily until day 11. This was concurrent with an increased uptake from the environment. Thus, the dynamics occurring in the levels of non-labelled total and ionic calcium together with the calcium uptake rates from the radiolabelled experiment, suggests an initial increase in calcium uptake from the environment, followed by the start of deposition of $CaCO_3$ onto the regenerate around day 4. Thereafter, the accumulation of radiolabelled calcium, as free calcium species at days 11 and 14, concomitant with continued $CaCO_3$ deposition, suggests an increased turn-over rate of free calcium from the environment onto the regenerating shell. A similar scenario, with indications for a rapid turnover of calcium in the mantle tissue during shell damage has previously been hypothesised for *C. virginica* (Wilbur and Jodrey, 1952).

Overall, total plasma calcium in *C. gigas* was mainly present in the ionic form (77–95%), with only minor parts bound to proteins or inorganic ligands. The present absolute values of ionic calcium are in line with previous data for the same species (Lannig et al., 2010) as well as for *Mytilus edulis* (Thomsen et al., 2010). However, those, as most previous studies, have not performed simultaneous measures of the different hemolymph calcium fractions, making it difficult to compare the results. In the quahog (*Mercenaria mercenaria*), the distribution of calcium into different fractions was performed using equilibrium dialysis (cut off 1 kDa), revealing the ionic calcium to constitute only 2% of the total plasma calcium (Nair and Robinson, 1999). The same study also used a calcium speciation computer modelling and the authors suggest that collectively the two methods show that most of the hemolymph

Table 3
Uptake of calcium in different tissues traced as radiolabelled ^{45}Ca. Asterisk (*) indicates significant difference between the two treatments and (#) indicates overall effect of time. Values expressed as μmol/g wet weight (± standard error of mean).

μmol/g		Day 1	Day 2	Day 4	Day 7	Day 11	Day 14
Mantle 1 #	Control	3.81 ± 0.23	4.40 ± 0.24	4.87 ± 0.27	5.92 ± 0.20	5.43 ± 0.65	5.76 ± 0.73
	Notched	4.47 ± 0.50	4.93 ± 0.42	6.63 ± 0.41	7.37 ± 1.67	5.41 ± 0.34	5.16 ± 0.26
Mantle 2 #*	Control	3.39 ± 0.30	3.91 ± 0.31	4.80 ± 0.20	6.07 ± 0.42	4.66 ± 0.38	5.90 ± 0.71
	Notched	4.41 ± 0.30	4.62 ± 0.38	5.00 ± 0.44	6.22 ± 0.49	4.98 ± 0.21	7.58 ± 0.57
Mantle 3 #*	Control	2.65 ± 0.44	2.55 ± 0.14	3.65 ± 0.32	4.20 ± 0.27	4.21 ± 0.46	3.92 ± 0.70
	Notched	3.81 ± 0.35	3.34 ± 0.24	4.12 ± 0.21	4.31 ± 0.24	4.61 ± 0.49	4.78 ± 0.31
Mantle 4 #	Control	3.66 ± 0.37	4.30 ± 0.23	4.66 ± 0.09	7.06 ± 0.91	5.21 ± 0.60	5.46 ± 0.57
	Notched	4.00 ± 0.37	4.82 ± 0.28	5.70 ± 0.37	5.84 ± 0.39	4.93 ± 0.41	5.06 ± 0.46
Mantle 5 #	Control	4.14 ± 0.26	4.08 ± 0.17	5.20 ± 0.34	5.92 ± 0.58	5.50 ± 0.55	5.03 ± 0.39
	Notched	4.04 ± 0.14	4.86 ± 0.38	5.31 ± 0.32	5.57 ± 0.30	5.04 ± 0.26	6.52 ± 0.54
Gills #	Control	1.18 ± 0.08	3.74 ± 0.24	4.92 ± 0.14	6.17 ± 0.46	5.08 ± 0.22	5.31 ± 0.50
	Notched	1.97 ± 0.33	4.76 ± 0.47	4.63 ± 0.83	5.70 ± 0.63	5.46 ± 0.21	6.39 ± 0.23
Muscle #	Control	1.25 ± 0.20	2.87 ± 0.42	3.73 ± 0.35	4.77 ± 0.55	4.22 ± 0.29	4.18 ± 0.28
	Notched	1.87 ± 0.30	4.41 ± 0.38	4.23 ± 0.41	4.59 ± 0.26	4.22 ± 0.32	4.56 ± 0.18

calcium was bound to organic ligands (Nair and Robinson, 1999). The use of different cut off sizes, 30 kDa versus 1 kDa, in the present study and the study on *M. mercenaria*, respectively could provide an explanation to the discrepancies between the two studies. However, in the present study, the ionic calcium in the hemolymph was analysed using ion selective electrodes, confirming that the majority of the free calcium in *C. gigas* is present in the ionic form.

In the present study, hemolymph protein bound calcium concentration was not affected by the induced shell damage, nor was the uptake to the protein bound species. Thus, in *C. gigas*, the calcium bound to proteins does not seem to act as a calcium reservoir during periods of increased calcium demands. This suggests that the ionic calcium levels are less tightly regulated and allowed to fluctuate in response to changes in uptake rates and rates of incorporation of calcium. This is in contrast to the situation in most vertebrates investigated, where the free and especially ionic calcium is tightly regulated by several hormonal factors, whereas the protein bound calcium is allowed to fluctuate and thus act as a buffer (McLean and Hastings, 1935; Dacke, 1979).

The general view is that oysters are osmoconformers and isosmotic with the environment. *C. gigas* exposed to abrupt changes in environmental salinity rapidly followed these changes in the hemolymph osmolality, experimentally supporting this hypothesis (Hosoi et al., 2003). In the present study, no major changes in water salinity or osmolality were observed during the experiment. In line with this, there were no major changes observed in plasma sodium levels with time or between the two treatment groups and these concentrations were also close to environmental sodium levels. For potassium, on the other hand, the hemolymph levels were found to be 52–125% higher than the environmental levels. This pattern was also shown in *C. gigas* by Alavi et al. (2014), where plasma concentrations of potassium and calcium were increased by 81% and 43% percent respectively compared to the environment. Furthermore, the potassium levels in the present

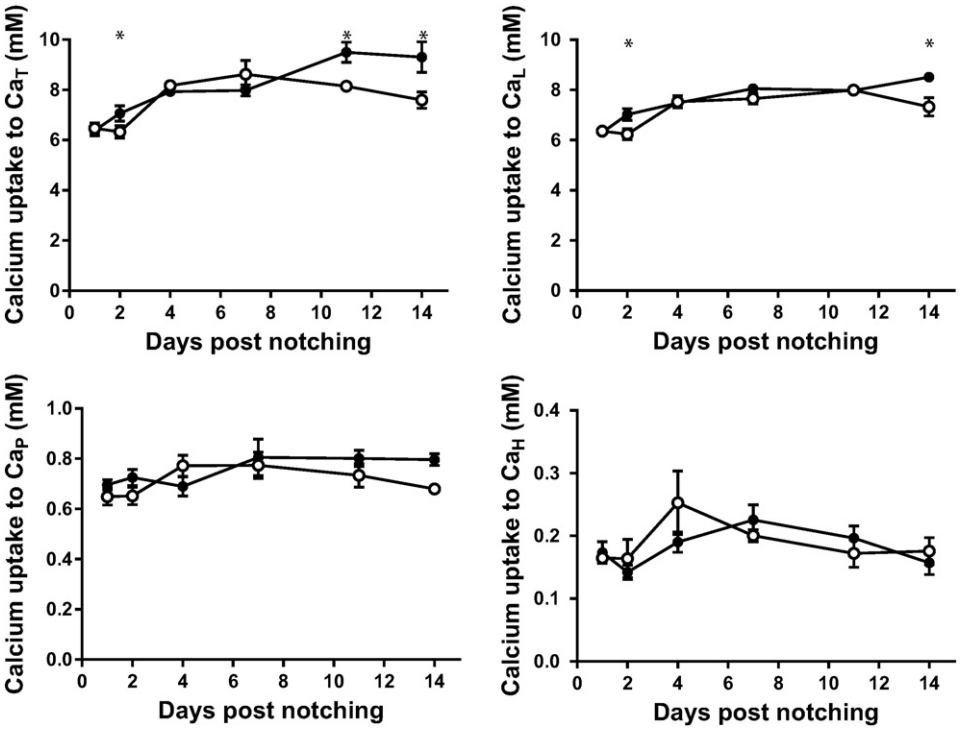

Fig. 6. The calcium uptake (mM) traced as ^{45}Ca into different calcium species in the hemolymph of notched and control oysters with time. A) total plasma calcium, Ca_T; B) calcium bound in complexes <30 kDa, Ca_L; C) calcium bound to proteins >30 kDa, Ca_P; D) calcium inside hemocytes, Ca_H. Values are means ± standard error of the mean (n = 6) and asterisks denotes significant differences between treatment groups ($p < 0.05$; Bonferroni multiple pairwise comparison).

study were consistently lower in the notched oyster than in the control. Taken together this suggests that *C. gigas* actively upregulates the potassium levels in the hemolymph. A similar pattern has been found in the blue mussel, *M. edulis*, were the hemolymph potassium levels varied between 117 and 135% of the seawater level (Thomsen et al., 2010). The reason for this upregulation of potassium needs further investigations. Additionally, the changes in hemolymph calcium concentrations during the shell regeneration process suggest calcium to be actively regulated above or below environmental levels. Taken together, the changes in potassium and calcium levels in the hemolymph suggest that the Pacific oyster may have the ability to regulate the extracellular levels of specific ions.

Induced shell damage increased calcium uptake in the upper mantle tissue area located near the notch (tissue 2) as well as in the lower mantle in the area opposite to the notch, near the hinge (tissue 3). Neither the lower mantle area closest to the notch (tissue 1), that was directly exposed to the environmental water, nor the gills showed elevated Ca uptake in notched compared to control oysters. Previous ^{45}Ca tracer studies on shell growth of *C. virginica*, have suggested a rapid (hours) transfer of calcium from seawater onto the shell (Jodrey, 1953). In *C. virginica*, the ^{45}Ca levels of the mantle tissue were greatly reduced compared to the levels found incorporated into the shell, which was interpreted as a rapid turn-over rate of ^{45}Ca in this species (Wilbur and Jodrey, 1952; Jodrey, 1953). A similar rapid turn-over of calcium from the environment in the mantle area 1 and the gills could explain the lack of significant elevation of ^{45}Ca in these regions, as the first sampling point in the present study was not until 24 h after the start of exposure. Overall, methodological differences in preparation, exposure time and sampling frequencies make it difficult to compare the different experiments. The present study was long term, using whole animals, a constant exposure to ^{45}Ca in the environment and relatively low resolution in sampling time, intervals of 24 h or more, whereas previous studies used fragments of shell and mantle and/or short exposure times and more frequent samplings (Wilbur and Jodrey, 1952; Akberali, 1980). Additionally, the oysters were not fed in the current study. Starvation of oysters can result in a switch to a more anaerobic metabolism and result in less cellular energy available, which may affect the overall calcium transport rate with time in both the control and notched oysters. However, the oyster species used in the present study, *C. gigas*, have been shown to contain large glycogen stores and to be tolerant to periods of starvation as long as 16 weeks (Dunphy et al., 2006).

Traditionally, bivalve hemocytes have been divided into two groups, hyalinocytes and granulocytes, though both of these can be further classified based on morphology (Hégaret et al., 2003a). Hemocytes have multiple functions such as nutrient transport, wound and shell repair, and gonad resorption. However, one of the main functions of hemocytes is their involvement in immune defence (Bachère et al., 2015). Induced shell damage has been reported to cause an increase in circulating hemocytes and promote hemocyte migration towards the inner mantle epithelium in the deep-sea vent mussel, *Bathymodiolus azoricus* (Kádár, 2008). The increase in hemocyte abundances observed in the present study may be due to mobilisation of hemocytes from the tissues, or due to synthesis of new hemocytes, as observed in the case of immune reactions (Allam et al., 2000). The role of hemocytes in immune defence makes it difficult to evaluate their exact role in the shell repair processes. Hemocyte counts have been noted to increase after bacterial infection in Manila clams (*Ruditapes philippinarum*; Allam et al., 2000) and soft-shelled clams (*Mya arenaria*; Mateo et al., 2009) with maximum numbers obtained at day 7 in *R. philippinarum* (Allam et al., 2000). In the present study, the peak in hemocyte count was observed at day 7 in the notched oysters. The number then decreased, though remained higher than the initial count throughout the experimental period. The number of granulocytes also increased throughout the experimental period in the notched oysters, albeit in a continuous pattern. Mount et al. (2004) noted that in *C. virginica* the proportion of refractive granulocytes, which contain calcite resembling crystals (REF granulocytes), increased from 5% to 15% of the total hemocyte populations 48 h after notching. The REF granulocytes were therefore suggested to play a major role in shell regeneration. In more recent investigations, Johnstone et al. (2015) suggested that hemocytes take part in shell formation together with the outer mantle epithelium and are involved in the regulation of the deposition of organic and mineral phases. The increases in hemocyte and granulocyte counts in the present study could be an indication of multiple hemocyte functions; in an immune response as well as contributing to shell regeneration. The lack of increased levels of calcium in hemocytes as well as the absence of increased ^{45}Ca uptake into hemocytes in the notched compared to control oyster contradicts a prominent role of granulocytes in $CaCO_3$ deposition during shell regeneration. However, there are methodological concerns regarding the analyses of both total and radiolabelled calcium in the hemocyte fractions. The intracellular concentrations of calcium inside the hemocytes are negligible compared to the concentrations in the hemolymph, making the hemocyte samples prone to contamination. Therefore, a role of the granulocytes in shell regeneration of *C. gigas* cannot be excluded at this point.

5. Conclusions

The present study suggests that induced shell damage results in a dynamic regulation of calcium uptake from the environment, starting with increased uptake directly after notching, followed by increased incorporation of calcium onto the regenerating shell around day 4 and a further increased uptake as well as deposition of calcium during days 11–14. Twenty four hours after notching, increased uptake of ^{45}Ca to upper mantle tissue near the notch and to lower mantle tissue near the hinge was apparent. Thus, there is a divergent calcium uptake to the mantle tissues in response to notching, but the relative importance of different mantle areas are difficult to assess due to the low time resolution at the beginning of the experiment. Furthermore, the notching evokes proliferation of hemocytes, which may be due to immune stimulation and/or a possible involvement in the shell regeneration.

Acknowledgements

The authors would like to thank L. Hasselberg Frank and S. Samuelsson for assistance with the sampling and analyses, and K. Elliot for proof reading of the manuscript. This study was funded by the Marie Curie Initial Training Networks (ITN) (Grant agreement 605051) and supported by a grant from Herbert & Karin Jacobssons Stiftelse to K. Sillanpää.

References

Addadi, L., Joester, D., Nudelman, F., Weiner, S., 2006. Mollusk shell formation: a source of new concepts for understanding biomineralization process. Chem. Eur. J. 12, 980–987.
Akberali, H.B., 1980. ^{45}Calcium uptake and dissolution in the shell of *Scrobicularia plana* (da costa). J. Exp. Mar. Biol. Ecol. 43 (1), 1–9.
Alavi, S.M., Matsumura, N., Shiba, K., Itoh, N., Takahashi, K.G., Inaba, K., Osada, M., 2014. Roles of extracellular ions and pH in 5-HT-induced sperm motility in marine bivalve. Reproduction 147 (3), 331–345.
Allam, B., Paillard, C., Auffret, M., 2000. Alterations in hemolymph and extrapallial fluid parameters in the Manila clam, *Ruditapes philippinarum*, challenged with the pathogen Vibrio tapetis. J. Invertebr. Pathol. 76 (1), 63–69.
Bachère, E., Rosa, R.D., Schmitt, P., Poirier, A.C., Merou, N., Charrière, G.M., Destoumieux-Garzón, D., 2015. The new insights into the oyster antimicrobial defense: cellular, molecular and genetic view. Fish Shellfish Immunol. 46, 50–64.
Burton, R.F., 1983. Ionic regulation and water balance. In: Wilbur, K.M., Saleuddin, A.S.M. (Eds.), The mollusca volume 5. Physiology Part 2, pp. 291–341.
Cavanaugh, G.M., 1975. Formulae and methods VI. The Marine Biological Laboratory, Woods Hole, MA, from Biological Bulletin Compendia.
Cho, S.M., Jeong, W.G., 2011. Prismatic shell repairs by hemoctyes in the extrapallial fluid of the Pacific oyster, *Crassostrea gigas*. Korean J. Malacology 27, 223–228.
Coimbra, A.M., Ferreira, K.G., Fernandes, P., Ferreira, H.G., 1993. Calcium exchanges in *Anodonta cygnea*: barriers and driving gradients. J. Comp. Physiol. B. 163 (3), 196–202.
Dacke, C.G., 1979. Calcium Regulation in Sub-Mammalian Vertebrates. Academic Press, London.

Dunphy, B.J., Wells, R.M.G., Jeffs, A.G., 2006. Oxygen consumption and enzyme activity of the subtidal flat oyster (*Ostrea chilensis*) and intertidal Pacific oyster (*Crassostrea gigas*): responses to temperature and starvation. N. Z. J. Mar. Freshw. Res. 40 (1), 149–158.

Eyster, L.S., 1983. Ultrastructure of early embryonic shell formation in the opisthobranch gastropod *Aeolidia papillosa*. Biol. Bull. 165, 394–408.

Fan, W., Li, C., Wang, X., Gong, N., Xie, L., Zhang, R., 2007. Cloning, characterization and expression analysis of calcium channel beta subunit from pearl oyster (*Pinctada fucata*). J. Biosci. Bioeng. 104 (1), 47–54.

Hégaret, H., Wikfors, G.A., Soudant, P., 2003a. Flow-cytometric analysis of haemocytes from eastern oysters, *Crassostrea virginica*, subjected to a sudden temperature elevation I. Haemocyte types and morphology. J. Exp. Mar. Biol. Ecol. 293 (2), 237–248.

Hégaret, H., Wikfors, G.A., Soudant, P., 2003b. Flow cytometric analysis of haemocytes from eastern oysters, *Crassostrea virginica*, subjected to a sudden temperature elevation II. Haemocyte functions: aggregation, viability, phagocytosis, and respiratory burst. J. Exp. Mar. Biol. Ecol. 293, 249–265.

Heinemann, A., Fietzke, J., Melzner, F., Böhm, F., Thomsen, J., Garbe-Schönberg, D., Eisenhauer, A., 2012. Conditions of *Mytilus edulis* extracellular body fluids and shell composition in a pH-treatment experiment: acid–base status, trace elements and δ^{11}B. Geochem. Geophys. Geosyst. 13 (1).

Hohagen, J., Jackson, D.J., 2013. An ancient process in a modern mollusc: early development of the shell in *Lymnaea stagnalis*. BMC Dev. Biol. 13, 27.

Horiguchi, Y., 1958. Biochemical studies on *Pteria* (Pinctada) *martensii* (Dubker) and *Hyriopsis schlegeli* (Martens). IV. Absorption and transference of ^{45}Ca in *Hyriopsis schlegeli* (Martens). Bull. Jpn. Soc. Sci. Fish. 23, 710–715.

Hosoi, M., Kubota, S., Toyohara, M., Toyohara, H., Hayashi, I., 2003. Effect of salinity change on free amino acid content in Pacific oyster. Fish. Sci. 69, 395–400.

Hüning, A., 2013. Responsiveness of *Mytilus edulis* Towards Mechanical Stress and Elevated pCO2—Combined Transcriptomic, Proteomic and Physiological Analyses. Universität Bremen PhD thesis.

Jodrey, L.H., 1953. Studies on shell formation. III. Measurement of calcium deposition in shell and calcium turnover in mantle tissue using the mantle-shell preparation and Ca^{45}. Biol. Bull. 104, 398–407.

Johnstone, M.B., Gohad, N.V., Falwell, E.P., Hansen, D.C., Mount, A.S., 2015. Cellular orchestrated biomineralization of crystalline composites on implant surfaces by the eastern oyster, *Crassostrea virginica* (Gmelin, 1791). J. Exp. Mar. Biol. Ecol. 463, 8–16.

Jokumsen, A., Fyhn, H.J., 1982. The influence of aerial exposure upon respiratory and osmotic properties of haemolymph from two intertidal mussels, Mytilus edulis L. and Modiolus modiolus. J. Exp. Mar. Biol. Ecol. 61, 189–203.

Joubert, C., Piquemal, D., Marie, B., Manchon, L., Pierrat, F., Zanella-Cléon, I., Cochennec-Laureau, N., Gueguen, Y., Montagnani, C., 2010. Transcriptome and proteome analysis of *Pinctada margaritifera* calcifying mantle and shell: focus on biomineralization. BMC Genomics 11 (1).

Kádár, E., 2008. Haemocyte response associated with induction of shell regeneration in the deep-sea vent mussel *Bathymodiolus azoricus* (Bivalvia: Mytilidae). J. Exp. Mar. Biol. Ecol. 362 (2), 71–78.

Kahl, S.D., Sitta Sittampalam, G., Weidner, J., 2012. Calculations and instrumentation used for radioligand binding assays. Assay Guidance Manual. National Center for Advancing Translational Sciences.

Kniprath, E., 1980. Larval development of the shell and the shell gland in *Mytilus* (Bivalvia). Wilhelm Rouxs Arch. Dev. Biol. 188, 201–204.

Lambert, C., Soudant, P., Degremont, L., Delaporte, M., Moal, J., Boudry, P., Jean, F., Huvet, A., Samain, J.F., 2007. Hemocyte characteristics in families of oysters, *Crassostrea gigas*, selected for differential survival during summer and reared in three sites. Aquaculture 270, 276–288.

Lannig, G., Eilers, S., Pörtner, H.O., Sokolova, I.M., Bock, C., 2010. Impact of ocean acidification on energy metabolism of oyster, *Crassostrea gigas* — changes in metabolic pathways and thermal response. Mar. Drugs 8 (8), 2318–2339.

Levi-Kalisman, Y., Falini, G., Addadi, L., Weiner, S., 2001. Structure of the nacreous organic matrix of a bivalve mollusk shell examined in the hydrated state using cryo-TEM. J. Struct. Biol. 135 (1), 8–17.

Marie, B., Zanella-Cleon, I., Guichard, N., Becchi, M., Marin, F., 2011. Novel proteins from the calcifying shell matrix of the Pacific oyster *Crassostrea gigas*. Mar. Biotechnol. (N.Y.) 13 (6), 1159–1168.

Marin, F., Luquet, G., 2004. Molluscan shell proteins. C.R. Palevol 3, 469–492.

Marin, F., Le Roy, N., Marie, B., 2012. The formation and mineralization of mollusk shell. Front. Biosci. (Schol. Ed.) 4 S (3), 1099–1125.

Mateo, D.R., Siah, A., Araya, M.T., Berthe, F.C.J., Johnson, G.R., Greenwood, S.J., 2009. Differential in vivo response of soft-shell clam hemocytes against two strains of *Vibrio splendidus*: changes in cell structure, numbers and adherence. J. Invertebr. Pathol. 102 (1), 50–56.

Matozzo, V., Marin, M.G., 2007. First evidence of altered vitellogenin-like protein level in clam *Tapes philippinarum* and in cockle *Cerastoderma glaucum* from the Lagoon of Venice. Mar. Pollut. Bull. 55, 494–504.

McLean, F.C., Hastings, A.B., 1935. Clinical estimation and significance of calcium-ion concentrations in the blood. Am. J. Med. Sci. 189, 601–613.

Medaković, D., 2000. Carbonic anhydrase activity and biomineralization process in embryos, larvae and adult blue mussels *Mytilus edulis* L. Helgol. Mar. Res. 54, 1–6.

Misogianes, M.J., Chasteen, N.D., 1979. A chemical and spectral characterization of the extrapallial fluid of *Mytilus edulis*. Anal. Biochem. 100, 324–334.

Miyazaki, Y., Nishida, T., Aoki, H., Samata, T., 2010. Expression of genes responsible for biomineralization of *Pinctada fucata* during development. Comp. Biochem. Physiol. B Biochem. Mol. Biol. 155 (3), 241–248.

Mount, A.S., Wheeler, A.P., Paradkar, R.P., Snider, D., 2004. Hemocyte-mediated shell mineralisation in the Eastern Oyster. Science 304, 297–300.

Nair, P.S., Robinson, W.E., 1998. Calcium speciation and exchange between blood and extrapallial fluid of the quahog *Mercenaria mercenaria* (L.). Biol. Bull. 195 (1), 43–51.

Nair, P.S., Robinson, W.E., 1999. Purification and characterization of a histidine-rich glycoprotein that binds cadmium from the blood plasma of the bivalve *Mytilus edulis*. Arch. Biochem. Biophys. 366 (1), 8–14.

Potts, W.T.W., 1967. Excretion in the molluscs. Biol. Rev. 42, 1–41.

Renwrantz, L., Schmalmack, W., Steenbuck, M., 1998. Molecular size of native proteins of *Mytilus* serum which contains a dominant fraction with heavy metal-binding properties. Comp. Biochem. Physiol. A Mol. Integr. Physiol. 121 (2), 175–180.

Rousseau, M., Plouguerné, E., Wan, G., Wan, R., Lopez, E., Fouchereau-Peron, M., 2003. Biomineralization markers during a phase of active growth in *Pinctada margaritifera*. Comp. Biochem. Physiol. 135, 271–278.

Suzuki, M., Saruwatari, K., Kogure, T., Yamamoto, Y., Nishimura, T., Kato, T., Nagasawa, H., 2009. An acidic matrix protein, Pif, is a key macromolecule for nacre formation. Science 325 (5946), 1388–1390.

Thomsen, J., Gutowska, M.A., Saphörster, J., Heinemann, A., Trübenbach, K., Fietzke, J., Hiebenthal, C., Eisenhauer, A., Körtzinger, A., Wahl, M., Melzner, F., 2010. Calcifying invertebrates succeed in a naturally CO_2-rich coastal habitat but are threatened by high levels of future acidification. Biogeosciences 7, 3879–3891.

Wheeler, A.P., Sikes, C.S., 1984. Regulation of carbonate calcification by organic matrix. Am. Zool. 24 (4), 933–944.

Wilbur, K.M., Jodrey, L.H., 1952. Studies on shell formation. I. Measurement of the rate of shell formation using Ca^{45}. Biol. Bull. 103 (2), 269–276.

Xiang, L., Kong, W., Su, J., Liang, J., Zhang, G., Xie, L., Zhang, R., 2014. Amorphous calcium carbonate precipitation by cellular biomineralization in mantle cell cultures of *Pinctada fucata*. PLoS One 9 (11).

Zhang, C., Zhang, R., 2006. Matrix proteins in the outer shells of molluscs. Mar. Biotechnol. (N.Y.) 8 (6), 572–586.